

Learning to Ground Visual Objects for Visual Dialog via Answer-Aware Knowledge Distillation

Feilong Chen^{1,2,4}, Xiuyi Chen^{1,2,4}, Shuang Xu¹ Bo Xu^{1,2,3,4}

¹Institute of Automation, Chinese Academy of Sciences (CASIA), Beijing, China.

²School of Future Technology, University of Chinese Academy of Sciences

³School of Artificial Intelligence, University of Chinese Academy of Sciences

⁴Research Center for Brain-inspired Intelligence, CASIA

{chenfeilong2018, chenxiuyi2017, shuang.xu, xubo}@ia.ac.cn

Abstract

Visual dialog is challenging since it needs to answer a series of coherent questions based on understanding the visual environment. How to ground related visual objects is one of the key problems. Previous studies utilize the question and history to attend to the image and achieve satisfactory performance, while these methods are not sufficient to locate related visual objects without any guidance. The inappropriate grounding of visual objects prohibits the performance of visual dialog models. In this paper, we propose a novel approach to Learn to Ground visual objects for visual dialog via answer-aware Knowledge Distillation (LGKD), which is achieved using a teacher-student framework. We regard previous models as the student that attends to related visual objects based on questions and history. Differently, we train the student to learn to ground visual objects with the guidance of a pretrained answer-aware teacher, which utilizes questions, answers, history to ground related visual objects. Experimental results on the VisDial v0.9 and v1.0 datasets demonstrate that our approach improves the previous strong models in both generative and discriminative settings by a significant margin.¹

1 Introduction

With the development of deep learning, various vision-language tasks have been introduced and attracted widespread attention, such as image captioning (Xu et al., 2015; Anderson et al., 2016, 2018; Cornia et al., 2020; Ghanimifard and Dobnik, 2019), visual question answering (Ren et al., 2015a; Gao et al., 2015; Lu et al., 2016; Anderson et al., 2018; Li et al., 2019; Huang et al., 2020) and visual dialog (Das et al., 2017; Kottur et al., 2018; Agarwal et al., 2020; Wang et al., 2020; Qi et al., 2020). Specifically, visual dialog, which aims to

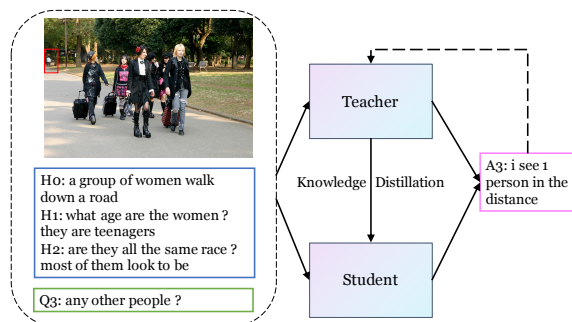


Figure 1: A motivating example of our approach. We see that the teacher with the access of answer can easily locate the visual object and transfer the Visual Grounding ability to the student via knowledge distillation.

hold a meaningful conversation with a human about a given image, is a challenging task that requires models to locate related visual objects in an image and answer the current question based on the history and the located visual objects.

In order to answer the question correctly, we need to accurately locate the question-related visual objects. Most existing methods utilize kinds of attention mechanism (Lu et al., 2017; Wu et al., 2018; Kottur et al., 2018; Gan et al., 2019; Guo et al., 2019b) to capture the target visual objects. ReDAN (Gan et al., 2019) and DMAM (Chen et al., 2020) use multi-step reasoning based on dual attention to iteratively update related visual objects. DAN (Guo et al., 2019b), MCAN (Agarwal et al., 2020) and LTMI (Nguyen et al., 2020) utilize multi-head attention mechanisms to manage multi-modal intersection and obtain weight distributions. Moreover, there are some approaches (Zheng et al., 2019; Schwartz et al., 2019; Jiang et al., 2020b; Guo et al., 2020; Jiang et al., 2020a) using graph-based structures to capture related visual objects. FGA (Schwartz et al., 2019) realizes a factor graph attention mechanism, which constructs the graph over all the multi-modal features and esti-

¹We will release the code at GitHub upon publication.

Model	w/o Ans	w/ Ans
LTMI (Nguyen et al., 2020)	68.6	97.1
Random	3.6	3.6
Human	96.7	99.3

Table 1: Accuracy of visual grounding with and without knowing the answer. We randomly sample 1000 samples and ask human annotators to ground the most likely object from the image.

mates their interactions to ground visual objects. CAG (Guo et al., 2020) focuses on an iterative question-conditioned context-aware graph to locate related visual objects.

However, the methods mentioned above obtain the distribution of visual objects through various interactions of questions, history and images, and finally use the distribution to obtain the final representation of the image. As shown in Figure 1, it becomes easier for us to ground the visual object (grounding by the red box) related the question “*any other people ?*” if we know the answer “*i see 1 person in the distance*”. The difficulty of grounding visual objects prevents the improvement of the model performance. We statistics the accuracy of visual grounding with and without knowing the answer as shown in Table 1. We find that the accuracy of grounding visual objects via LTMI (Nguyen et al., 2020) is 68.6 while the accuracy is 97.1 when LTMI additionally uses the answers to ground visual objects, which exceeds the accuracy of 96.7 when human ground visual objects without answers. As we expect, answers can improve the accuracy of visual grounding. Thus, we propose answer-aware knowledge distillation to utilize answers to make models learn to ground visual objects.

In this paper, we propose a method to learn to ground visual objects in visual dialog based on a teacher-student framework. Specifically, the student is as the same as existing visual dialog models which take questions, history and images as inputs. The teacher equipped with answers additionally learns how to ground answer-aware visual objects and then guides the student via knowledge distillation. During inference, the student will be applied. We test the effectiveness of our proposed model on two large-scale datasets: VisDial v0.9 and v1.0 (Das et al., 2017). Both automatic and manual evaluations show that our approach can be used to improve the strong baseline LTMI (Nguyen

et al., 2020). The contributions of this work are summarized as follows:

- We explore the importance of answers in grounding visual objects related to questions in visual dialog.
- We propose a novel answer-aware knowledge distillation approach based on teacher-student framework to realize learning to ground visual objects in visual dialog.
- We conduct extensive experiments and ablation studies on two large-scale datasets VisDial v0.9 and v1.0. Experimental results show that our approach can be used to improve previous visual dialog models in both generative and discriminative settings.

2 Methodology

2.1 Model Architecture

According to Das et al. (2017), a visual dialog agent takes an image i , history (the caption and question-answer pairs) till round $t - 1$: $h = (\underbrace{Cap}_{h_0}, \underbrace{(q_1, a_1)}_{h_1}, \dots, \underbrace{(q_{t-1}, a_{t-1})}_{h_{t-1}})$ and the current question q_t at round t as inputs. Note that Cap is the caption describing the image taken as h_0 and h_1, \dots, h_{t-1} are concatenations of question-answer pairs. Visual dialog agent aims to predict an answer a_t to the question q_t . To pinpoint accurate visual objects for question answering, we design a teacher-student framework to construct visual object distribution as follows:

As shown in Figure 2, the bottom half is the student, which learns to attend to the image based on questions and history. The top half is the teacher, which ground related visual objects via utilize questions, answers and history. In practice, we design two methods to teach the student to learn the ability of answer-aware visual grounding, attention-based learning and representation-based learning.

2.2 Base Model

We take the strong baseline LTMI (Nguyen et al., 2020) as a base model to introduce our approach, which mainly consists of the following components:

Textual Encoder: We use two bi-directional LSTM encoders to extract token-level representations $\mathbf{Q} \in \mathbb{R}^{\lambda \times d_q}$ and $\mathbf{A} \in \mathbb{R}^{\lambda \times d_q}$ of the question

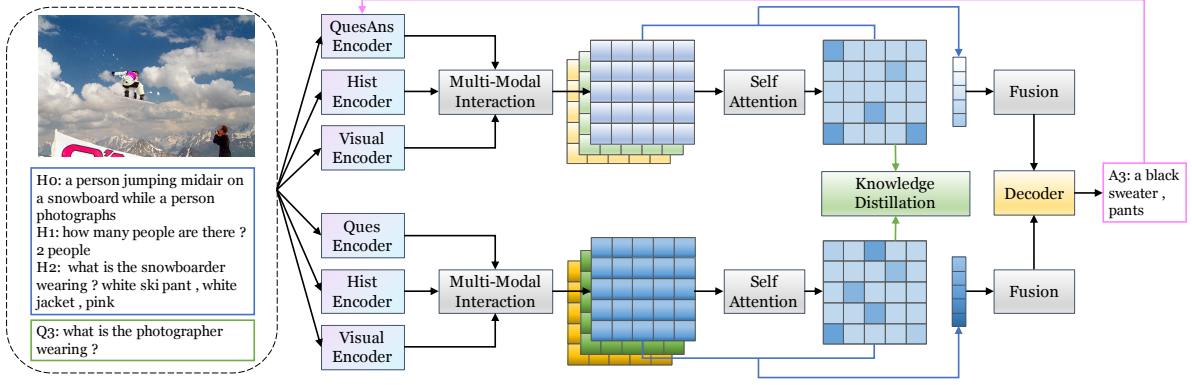


Figure 2: Framework of our Learning to Ground Visual Objects via Answer-Aware Knowledge Distillation. The top half is the teacher model which learns answer-aware visual grounding, and the bottom half is the student model which learns to ground visual objects with the guidance of the teacher via knowledge distillation. We omit some operation for the question features and history features.

q_t and the answer a_t . We use another bi-directional LSTM encoder to extract sentence-level representations $\mathbf{H} \in \mathbb{R}^{T \times d_q}$ of the history h . λ is the length of questions and answers with paddings, T is the turn of dialog and d_q is the dimension.

Visual Encoder: Similar to (Anderson et al., 2018), we extract the image features by using a pretrained Faster RCNN (Ren et al., 2015b). We select μ object proposals for each image, where each object proposal is represented by a 2048-dimension feature vector. We transform the obtained visual region features by a multi-layer perceptrons and obtain the image features $\mathbf{I} = \mathbf{I}_{I=0}^\mu \in \mathbb{R}^{\mu \times d_q}$.

Multi-modal Interaction: We use multi-head attention (Vaswani et al., 2017) to manage the multi-modal interaction. A cross-attention layer is firstly applied to outputs of the textual and visual encoders:

$$\mathbf{P} = \text{softmax}(\mathbf{I}\mathbf{Q}^T) \in \mathbb{R}^{\mu \times \lambda}, \quad (1)$$

$$\mathbf{I}_Q = \text{CrossAttn}(\mathbf{I}, \mathbf{Q}) = \mathbf{P}\mathbf{Q} \in \mathbb{R}^{\mu \times d_q}, \quad (2)$$

where the softmax conducts the normalization over each column of the matrix. We obtain the representation $\mathbf{Q}_H, \mathbf{Q}_I, \mathbf{Q}_Q, \mathbf{H}_Q, \mathbf{H}_I, \mathbf{H}_H, \mathbf{I}_H, \mathbf{I}_I$ as the same as the representation \mathbf{I}_Q . Then multi-layer perceptrons and layernorm operation are applied to the obtained representation as follows:

$$\bar{\mathbf{I}} = \text{MLP}([\mathbf{I}_Q, \mathbf{I}_H, \mathbf{I}_I]) \in \mathbb{R}^{\mu \times d_q}, \quad (3)$$

$$\hat{\mathbf{I}} = \text{LayerNorm}(\bar{\mathbf{I}}) \in \mathbb{R}^{\mu \times d_q}, \quad (4)$$

where MLP denotes the multi-layer perceptrons and $[\cdot, \cdot, \cdot]$ indicates concatenation. We obtain the

representation $\hat{\mathbf{Q}}, \hat{\mathbf{H}}$ as the same way as we calculate the representation $\hat{\mathbf{I}}$. We utilize $\hat{\mathbf{Q}}, \hat{\mathbf{H}}, \hat{\mathbf{I}} = \text{MultiAttn}(\mathbf{Q}, \mathbf{H}, \mathbf{I})$ to denote the Multi-modal Interaction.

Multi-modal Fusion: We convert the representation $\hat{\mathbf{Q}}, \hat{\mathbf{H}}, \hat{\mathbf{I}}$ into d_q -dimension vectors $\tilde{\mathbf{Q}}, \tilde{\mathbf{H}}, \tilde{\mathbf{V}}$. This conversion is performed by a simple self-attention computation as follows:

$$\mathbf{g} = \text{softmax}(\text{ReLU}(\hat{\mathbf{I}}\mathbf{W}_1 + \mathbf{b}_1)\mathbf{W}_2 + \mathbf{b}_2), \quad (5)$$

where $\mathbf{g} \in \mathbb{R}^{\mu \times 1}$, $\mathbf{W}_1, \mathbf{W}_2, \mathbf{b}_1, \mathbf{b}_2$ are learned parameters. We obtain the representation \mathbf{V} as follows:

$$\mathbf{V} = \mathbf{g}^T \hat{\mathbf{I}} \in \mathbb{R}^{d_q}, \quad (6)$$

We obtain the representation $\tilde{\mathbf{Q}}, \tilde{\mathbf{H}}$ as the same way as we obtain the representation \mathbf{V} . Then we obtain the final multi-modal representation as follows:

$$\mathbf{E} = \text{ReLU}([\tilde{\mathbf{Q}}, \tilde{\mathbf{H}}, \mathbf{V}]\mathbf{W}_3 + \mathbf{b}_3)\mathbf{W}_4 + \mathbf{b}_4, \quad (7)$$

where $\mathbf{E} \in \mathbb{R}^{d_q}$, $\mathbf{W}_3, \mathbf{W}_4, \mathbf{b}_3, \mathbf{b}_4$ are learned parameters.

Generative and Discriminative Decoder: We utilize another LSTM as our discriminative and generative decoders following the previous studies (Das et al., 2017; Nguyen et al., 2020). Receiving the final multi-modal representation \mathbf{E} and the candidate answers, the two decoders compute the score of each candidate answer in different ways. The objective function of the base model is to minimize the negative log-likelihood \mathcal{L}_G of answer generated for the generative decoder or the cross-entropy loss \mathcal{L}_D for the discriminative decoder.

2.3 Teacher Model

To ingest accurately related visual objects for question answering under the aforementioned base model, our teacher model builds an answer-aware visual object weight distribution $\mathbf{G} \in \mathbb{R}^{\mu \times 1}$ given the question features \mathbf{Q} , the history features \mathbf{H} and the image features \mathbf{I} , the answer features \mathbf{A} , then refines the interactional image features $\hat{\mathbf{I}}$ with \mathbf{G} . Elements in \mathbf{G} 's indicate the importance of visual objects in the image, with consideration of the answer.

Given the question features \mathbf{Q} , the history features \mathbf{H} and the image features \mathbf{I} , the answer features \mathbf{A} , we calculate the answer-aware question features:

$$\mathbf{Q}_A = \mathbf{Q} + \mathbf{A} \in \mathbb{R}^{\lambda \times d_q}. \quad (8)$$

Secondly, we calculate the representation $\hat{\mathbf{Q}}_A, \hat{\mathbf{H}}_A, \hat{\mathbf{I}}_A$ after conducting multi-modal interaction:

$$\hat{\mathbf{Q}}_A, \hat{\mathbf{H}}_A, \hat{\mathbf{I}}_A = \text{MultiAttn}(\mathbf{Q}_A, \mathbf{H}, \mathbf{I}). \quad (9)$$

Thirdly, we utilize $\hat{\mathbf{I}}_A$ to obtain the answer-aware visual object weight distribution \mathbf{G} :

$$\mathbf{G} = \text{softmax}(\text{ReLU}(\hat{\mathbf{I}}_A \mathbf{W}_{T1} + \mathbf{b}_{T1}) \mathbf{W}_{T2} + \mathbf{b}_{T2}), \quad (10)$$

where $\mathbf{W}_{T1}, \mathbf{W}_{T2}, \mathbf{b}_{T1}, \mathbf{b}_{T2}$ are learned parameters. We use \mathbf{G} to refine the interactional image representation $\hat{\mathbf{I}}_A$:

$$\mathbf{V}_A = \mathbf{G}^T \hat{\mathbf{I}}_A. \quad (11)$$

To avoid exposure bias of ground-truth answers (Sutskever et al., 2014), we calculate the representation $\tilde{\mathbf{Q}}_{Tech}, \tilde{\mathbf{H}}_{Tech}, \tilde{\mathbf{I}}_{Tech}$ after conducting multi-modal interaction without accessing the answer:

$$\tilde{\mathbf{Q}}_{Tech}, \tilde{\mathbf{H}}_{Tech}, \tilde{\mathbf{I}}_{Tech} = \text{MultiAttn}(\mathbf{Q}, \mathbf{H}, \mathbf{I}). \quad (12)$$

We obtain the interactional question representation $\tilde{\mathbf{Q}}_{Tech}$ and history representation $\tilde{\mathbf{H}}_{Tech}$ using $\tilde{\mathbf{Q}}_{Tech}$ and $\tilde{\mathbf{H}}_{Tech}$ as described in Eq. (5) and Eq. (6). Finally we obtain the final multi-modal representation \mathbf{E}_{Tech} to be sent to the decoder:

$$\mathbf{E}_A = \text{ReLU}([\tilde{\mathbf{Q}}_{Tech}, \tilde{\mathbf{H}}_{Tech}, \mathbf{V}_A] \mathbf{W}_{T3} + \mathbf{b}_{T3}) \mathbf{W}_{T4} + \mathbf{b}_{T4}, \quad (13)$$

where $\mathbf{W}_{T3}, \mathbf{W}_{T4}, \mathbf{b}_{T3}, \mathbf{b}_{T4}$ are learned parameters. The objective function of the teacher model is to minimize the negative log-likelihood \mathcal{L}_G of answer generated for the generative decoder or the cross-entropy loss \mathcal{L}_D for the discriminative decoder.

2.4 Learning to Ground Visual Objects

In this paper, we propose a novel approach to learn to ground visual objects, which is a significant problem but usually ignored in visual dialog. In this section, we introduce how the teacher teaches the student how to ground visual objects.

The student aims to exploit questions, history and images to answer question. Thus, any visual dialog models can be regarded as our student model. Here, we take the strong model LTMI (Nguyen et al., 2020) described in Section 2.2 as our student model to describe our approach. The student learns the visual object distribution \mathbf{g}_{Stu} described in Eq. (5) and the image representation \mathbf{V}_{Stu} described in Eq. (6). In the following, we describe two methods to teach the student to learn the ability of visual grounding.

Attention-based Learning. Learning the ability of visual grounding means that the student can decide the importance of each visual object just like the teacher. We narrow the the gap between the teacher's posterior visual object distribution \mathbf{G} and the student's prior visual object distribution \mathbf{g}_{Stu} to teach the student. We utilize the Kullback-Leibler (KL) divergence loss to narrow the the gap. The objective functions of the student are as follows:

$$\mathcal{L}_{GS} = \mathcal{L}_G + \lambda \mathcal{L}_{KL}(\mathbf{G}, \mathbf{g}_{Stu}), \quad (14)$$

$$\mathcal{L}_{DS} = \mathcal{L}_D + \lambda \mathcal{L}_{KL}(\mathbf{G}, \mathbf{g}_{Stu}), \quad (15)$$

$$\mathcal{L}_S = \mathcal{L}_G + \mathcal{L}_D + \lambda \mathcal{L}_{KL}(\mathbf{G}, \mathbf{g}_{Stu}), \quad (16)$$

where \mathcal{L}_{GS} is for the generative setting, \mathcal{L}_{DS} for the discriminative setting and \mathcal{L}_S for the multi-task setting.

Representation-based Learning. Besides learning the distribution, we can directly exploit the image representation to diminish the difference between the teacher and the student. Thus, we utilize the mean squared loss to diminishes the gap between the images representation \mathbf{V}_{Stu} and \mathbf{V}_A in the student model and the teacher model. Accordingly, the objective functions of the student change as follows:

$$\mathcal{L}_{GS} = \mathcal{L}_G + \lambda \mathcal{L}_{MSE}(\mathbf{V}_A, \mathbf{V}_{Stu}), \quad (17)$$

$$\mathcal{L}_{DS} = \mathcal{L}_D + \lambda \mathcal{L}_{MSE}(\mathbf{V}_A, \mathbf{V}_{Stu}), \quad (18)$$

$$\mathcal{L}_S = \mathcal{L}_G + \mathcal{L}_D + \lambda \mathcal{L}_{MSE}(\mathbf{V}_A, \mathbf{V}_{Stu}), \quad (19)$$

Model Training. We firstly train the teacher model until it converges, and then train the student model with the guidance of \mathbf{G} or \mathbf{V}_A from the

Model	VisDial v0.9 (val)					VisDial v1.0 (val)					
	MRR \uparrow	R@1 \uparrow	R@5 \uparrow	R@10 \uparrow	Mean \downarrow	NDCG \uparrow	MRR \uparrow	R@1 \uparrow	R@5 \uparrow	R@10 \uparrow	Mean \downarrow
MN (Das et al., 2017)	52.59	42.29	62.85	68.88	17.06	51.86	47.99	38.18	57.54	64.32	18.60
HCIAE (Lu et al., 2017)	53.86	44.06	63.55	69.24	16.01	59.70	49.07	39.72	58.23	64.73	18.43
CorefNMN (Kottur et al., 2018)	53.50	43.66	63.54	69.93	15.69	-	-	-	-	-	-
CoAtt (Wu et al., 2018)	54.11	44.32	63.82	69.75	16.47	59.24	49.64	40.09	59.37	65.92	17.86
RvA (Niu et al., 2019)	55.43	45.37	65.27	<u>72.97</u>	<u>10.71</u>	-	-	-	-	-	-
DVAN (Guo et al., 2019b)	55.94	<u>46.58</u>	65.50	71.25	14.79	-	-	-	-	-	-
Primary (Guo et al., 2019a)	-	-	-	-	-	-	49.01	38.54	59.82	66.94	16.60
ReDAN (Gan et al., 2019)	-	-	-	-	-	60.47	50.02	40.27	59.93	66.78	17.40
DMRM (Chen et al., 2020)	<u>55.96</u>	46.20	<u>66.02</u>	72.43	13.15	-	50.16	40.15	60.02	67.21	15.19
DAM (Jiang et al., 2020c)	-	-	-	-	-	60.93	<u>50.51</u>	<u>40.53</u>	<u>60.84</u>	67.94	16.65
VDBERT (Wang et al., 2020) \diamond	55.95	46.83	65.43	72.05	13.18	-	-	-	-	-	-
KBGN (Jiang et al., 2020a)	-	-	-	-	-	60.42	50.05	40.40	60.11	66.82	17.54
LTMI (Nguyen et al., 2020) \dagger	55.85	46.07	65.97	72.44	14.17	<u>61.61</u>	50.38	40.30	60.72	<u>68.44</u>	<u>15.73</u>
LTMI-LGKD (Ours)	56.56	46.71	66.69	73.37	13.62	63.23	51.30	41.34	61.61	69.06	15.26
LTMI-LGKD* (Ours)	56.59	46.87	66.92	73.76	13.35	63.53	51.43	41.68	61.96	69.87	14.89

Table 2: Main comparisons on both VisDial v0.9 and v1.0 datasets using the generative decoder. \dagger denotes that we re-implemented the model using the released code. \diamond denotes that the model utilizes large extra datasets for training which is unfair compared with other models. Underline indicates the highest performance among previous approaches except pretraining-base models. Our approach improves the strong baseline a lot. (t-test, p-value<0.01)

converged teacher model. Therefore, the student is able to learn the ability of visual grounding with the guidance of the teacher, which locates visual object more accurately. For inference, only the student model will be used to generate the output answer or score the candidate answers.

3 Experiments

3.1 Experiment Setup

Datasets. Our experiments are conducted on the VisDial v0.9 and v1.0 datasets (Das et al., 2017). VisDial v0.9 contains 1.23M dialog question-answer pairs totally with 83k dialog for training and 40k dialogs for validation. VisDial v1.0 dataset is an extension of VisDial v0.9 dataset, which contains 123k, 2k, and 8k images as train, validation, and test splits, respectively.

Implementation Details. A Faster R-CNN (Ren et al., 2015b) with ResNet-101 (He et al., 2016) finetuned on the Visual Genome dataset (Krishna et al., 2017) are used to represent image regions. We set $\mu = 100$ regions from each image and we use a 2048-dimension feature vector for each region.

Automatic Evaluation. To be consistent with previous work (Das et al., 2017; Chen et al., 2021a,b), we use a retrieval setting to evaluate individual responses at each round of a dialog. Specifically, there is a list of 100-candidate answers to be given at test time. We evaluate visual dialog models on retrieval metrics: (1) Rank of human response (the lower the better), (2) Existence of the human response in $top - k$ ranked responses, i.e.,

R@ k (the higher the better) (3) Mean Reciprocal Rank (MRR) of the human response (the higher the better) and (4) Normalized Discounted Cumulative Gain (NDCG, the higher the better) for VisDial v1.0.

Human Evaluation. Following (Wu et al., 2018; Chen et al., 2021a), we randomly extract 100 predicted samples for human evaluation. We ask 3 human subjects to guess whether the last response in the dialog is human-generated or machine-generated. If at least 2 of them agree it is generated by a human, we think it passes the Turing Test (M1). We record the percentage of responses that are evaluated better than or equal to human responses (M2), according to the human subjects' evaluation.

3.2 Main Results

Baseline methods. In our experiment, compared methods can be grouped into four types: (1) Fusion-based models: LF (Das et al., 2017) and HREA (Das et al., 2017). (2) Attention-based models: HCIAE (Lu et al., 2017), CoAtt (Wu et al., 2018), Primary (Guo et al., 2019a), ReDAN (Gan et al., 2019), CorefNMN (Kottur et al., 2018), RvA (Niu et al., 2019), DVAN (Guo et al., 2019b) and DMRM (Chen et al., 2020), DAM (Jiang et al., 2020c). (3) The pretraining model: VDBERT (Wang et al., 2020) and VisualBERT (Murahari et al., 2020). (4) Graph-based models: GNN (Zheng et al., 2019), DualVD (Jiang et al., 2020b), FGA (Schwartz et al., 2019), KBGN (Jiang et al., 2020a). Please refer to Appendix A.3 for

Model	VisDial v0.9 (val)					VisDial v1.0 (test-std)					
	MRR \uparrow	R@1 \uparrow	R@5 \uparrow	R@10 \uparrow	Mean \downarrow	NDCG \uparrow	MRR \uparrow	R@1 \uparrow	R@5 \uparrow	R@10 \uparrow	Mean \downarrow
ReDAN (Gan et al., 2019)	-	-	-	-	-	57.63	64.75	51.10	81.73	90.90	3.89
MCA (Agarwal et al., 2020)	-	-	-	-	-	<u>72.73</u>	37.68	20.67	56.67	72.12	8.89
GNN-EM (Zheng et al., 2019)	62.85	48.95	79.65	88.36	4.57	52.82	61.37	47.33	77.98	87.83	4.57
DualVD (Jiang et al., 2020b)	62.94	48.64	80.89	89.94	4.17	56.32	63.23	49.25	80.23	89.70	4.11
FGA (Schwartz et al., 2019)	65.25	51.43	82.08	89.56	4.35	56.90	<u>66.20</u>	<u>52.75</u>	<u>82.92</u>	<u>91.07</u>	<u>3.80</u>
CAG (Guo et al., 2020)	<u>67.56</u>	<u>54.64</u>	<u>83.72</u>	<u>91.48</u>	<u>3.75</u>	56.64	63.49	49.85	80.63	90.15	4.11
KBGN (Jiang et al., 2020a)	-	-	-	-	-	57.60	64.13	50.47	80.70	90.16	4.08
VisualBERT (Murahari et al., 2020) \diamond	-	-	-	-	-	74.47	50.74	37.95	64.13	80.00	6.28
VDBERT (Wang et al., 2020) \diamond	70.04	57.79	85.34	92.68	4.04	75.35	51.17	38.90	62.82	77.98	6.69
LTMI (Nguyen et al., 2020) \dagger	66.41	53.36	82.53	90.54	4.03	60.92	60.65	47.00	77.03	87.75	4.90
LTMI-LGKD (Ours)	67.63	54.69	83.74	91.38	3.75	58.55	64.00	50.63	80.58	90.20	4.12

Table 3: Main comparisons on both VisDial v0.9 and v1.0 datasets using the discriminative decoder. \diamond denotes that the model utilizes large extra datasets for training which is unfair compared with other models. Underline indicates the highest performance among previous approaches except the pretraining-based models. Our approach improves the strong baseline significantly. (t-test, p-value<0.01)

Model	NDCG	MRR	R@1	R@5	R@10	Mean
MN (Das et al., 2017)	-	60.29	46.14	77.68	87.57	4.84
HCIAE (Lu et al., 2017)	-	61.96	48.25	78.97	88.43	4.56
CoAtt (Wu et al., 2018)	-	62.77	49.38	78.99	88.49	4.56
ReDAN (Gan et al., 2019)	-	64.29	50.65	81.29	90.17	4.10
KBGN (Jiang et al., 2020a)	59.08	<u>64.86</u>	<u>51.37</u>	<u>81.71</u>	<u>90.54</u>	<u>4.00</u>
VDBERT (Wang et al., 2020) \ddagger	56.20	62.25	48.16	79.57	89.01	4.31
VDBERT (Wang et al., 2020) \diamond	63.22	67.44	54.02	83.96	92.33	3.53
LTMI (Nguyen et al., 2020) \dagger	<u>62.72</u>	62.32	48.94	78.65	87.88	4.86
LTMI-LGKD (Ours)	59.67	65.03	51.69	81.49	90.32	4.02

Table 4: Main comparisons on VisDial v1.0 val datasets using the discriminative decoder. \diamond denotes that the model utilizes large extra datasets for training. \ddagger denotes that the model trains from scratch.

Model	NDCG	MRR	R@1	R@5	R@10	Mean
LTMI \dagger	61.61	50.38	40.30	60.72	68.44	15.73
LGKD-Attn-MSE	63.03	51.14	40.91	61.78	69.43	15.08
LGKD-Image-MSE	62.80	51.21	41.01	62.02	69.90	14.90
LGKD-Attn-KL	63.23	51.30	41.34	61.61	69.06	15.26
LGKD-Image-KL	62.36	51.24	41.19	61.73	69.31	15.13
Attn-KL-Image-MSE	62.73	51.19	40.97	61.80	69.43	15.10

Table 5: Ablation study on VisDial v1.0 val datasets using the generative decoder.

more compared methods.

We realize our model LTMI-LGKD based on the strong baseline LTMI (Nguyen et al., 2020)². LTMI is a very strong model which achieves some the-state-of-the-art results. In general, our approach brings a large improvement to the strong baseline LTMI, which shows the effectiveness of our answer-aware knowledge distillation. We use t-test and analysis of variance (ANOVA) to analyze our model and LTMI. The p-values of these two analytical methods are all less than 0.01, indicating that the results are significantly different.

²We reproduce the result for LTMI by their official GitHub repo (<https://github.com/davidnvq/visdial>). We apply the default hyper-parameters as them.

Generative Results. As shown in Table 2, we compare the generative performance among different methods on the VisDial v1.0 val and VisDial v0.9 val. With the guidance of the teacher, we train our LTMI-LGKD with the ability of accurately grounding visual objects. As a result, our approach improve significantly (nearly 1% on all metrics) compared with LTMI (Nguyen et al., 2020). Comparing with the state-of-the-art results of different metrics, our model improves NDCG for 61.51 to 63.53 (+1.92), MRR from 50.51 to 51.43 (+0.92), R@1 from 40.53 to 41.68 (+1.13), R@5 from 60.84 to 61.96 (+1.12), R@10 from 68.44 to 69.87 (+1.43), Mean from 15.73 to 14.89 (+0.84) on the VisDial v1.0 val. Our model also brings a large improvement to LTMI (Nguyen et al., 2020) on the VisDial v0.9 val. The performance of our model exceeds the performance of VDBERT (Wang et al., 2020) \diamond on all the metrics except Mean. As we all know, we believe data is an important factor in deep learning (LeCun et al., 2015). VDBERT (Wang et al., 2020) \diamond works because it uses a lot of extra data for training. The reason why our method is effective is that we use the teacher to teach the student visual grounding, which can be regarded as a kind of data annotation.

Discriminative Results. As shown in Table 3 and Table 4, we compare our method with previous works on the VisDial v1.0 test, VisDial v0.9 val and VisDial v1.0 val. Our model improves significantly compared with LTMI (Nguyen et al., 2020), improving about +3% on MRR, R@1, R@5 and R@10 on the VisDial v1.0 test. Our approach also brings a large improvement on the Visdial v0.9 and achieves the best results on MRR, R@1

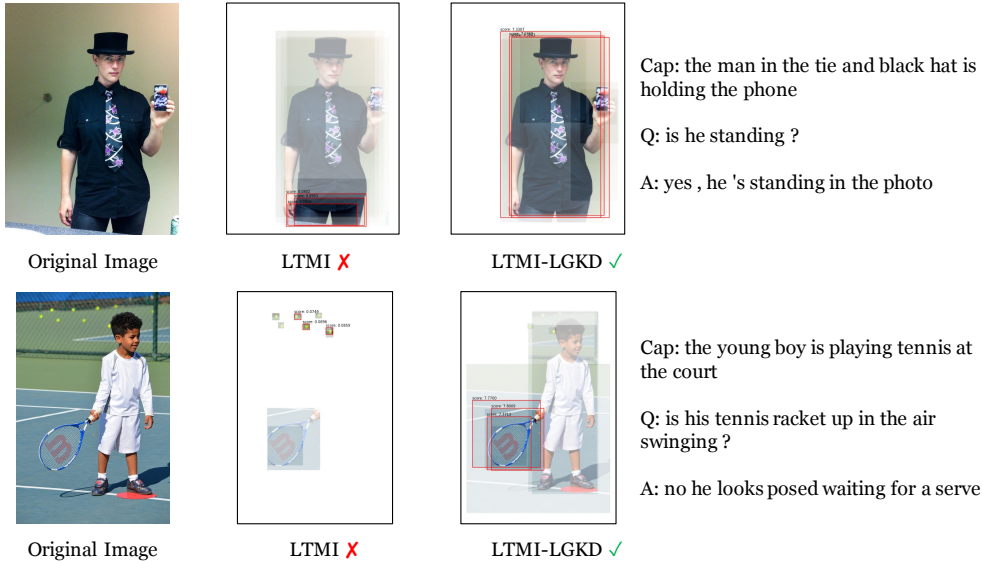


Figure 3: Visualization of attention maps generated by LTMI and our approach. Our approach grounds the related visual objects more accurately than LTMI.

and R@5 among non-pretrained models. In discriminative setting, our approach performs worse than pre-training models VisualBERT (Murahari et al., 2020)[◊] and VDBERT (Wang et al., 2020)[◊] because pre-training models utilize extra large-scale datasets to train the models which are unfair compared with other models. As shown in Table 4, VDBERT[‡] which trains from scratch performs worse than our LTMI-LGKD.

3.3 Ablation Study

In order to transfer knowledge, we need use some metric method to measure the gap between teachers and students. In our main experiments, we utilize the kullback-leibler (KL) divergence loss to diminish the gap of the weight distribution between the student model and the teacher model, the mean squared loss to diminish the gap of the representation of images. To compare different metric method, we utilize the mean squared loss for attention maps and KL loss for the representation of images as shown in Table 5. We find that KL loss is more suitable for attention distribution (better for NDCG, MRR and R@1) and MSE loss for the representation (better for R@5, R@10 and Mean). In addition, we use the attention via KL loss and the representation via MSE loss for distillation at the same time. The result is not so satisfactory and we think these two methods have some redundancy.

3.4 Case Study

As shown in Figure 3, we visualize the learned attention maps as an intuitive way to understand the

model. The colorful region means higher attention weights. We draw the bounding boxes of the first three highest scores. As shown in the top image in Figure 3, the question “is he standing ?” indicates the man’s overall posture rather than the local. LTMI grounds the wrong visual objects while our model grounds the right objects. As shown in the bottom image in Figure 3, the question “is his tennis racket up in the air swinging ?” concerns the racket rather than the tennis. Our model grounds accurately while LTMI makes mistakes. These examples show that our LTMI-LGKD has learned the ability of grounding visual objects via our answer-aware knowledge distillation. Moreover, similar to Table 1, we statistic the accuracy of grounding visual objects of our LTMI-LGKD, which is 82.1%. Our answer-aware knowledge distillation improves the accuracy from 68.6% (LTMI) to 82.1% (LTMI-LGKD), gaining 13.5% improvement. As shown in Figure 4, we provide predicted answers by LTMI and our LTMI-LGKD. Due to the improvement of visual grounding, our approach improves the generative and retrieval results of LTMI, managing to locate visual objects more accurately.

3.5 Human Study

As shown in Table 6, we conduct human study to further prove the effectiveness of our model. Our model achieves the highest scores both on the metric M1 and M2 compared with the previous model, LTMI (Nguyen et al., 2020). These results show that our model can generate a better contextually and visually coherent response.



a teenage girl in with long curly red hair who is on the phone

Question	Ground Truth	Generati on by LTMI-LGKD	Generatio n by LTMI	Retrieval by LTMI-LGKD	Retrieval by LTMI
Q1: what kind of phone ?	a cell phone	looks flip phone	looks flip phone	a cell phone	ca n't tell
Q2: what color is the phone ?	it is black	black	black 's black	it is black	it 's black
Q3: what color is the girl 's shirt ?	white	white	it	white or light blue shirt	there is n't 1
Q4: does she have a coat on ?	no she does n't	no she does n't	no	no she does n't	no
Q5: is it sunny ?	yes	yes	yes it sunny	yes	yes it is

Figure 4: Examples of dialogs generated and retrieved by our model and the LTMI baseline. Our model provides answers that are more accurate than LTMI (green denotes correct answers, and red denotes wrong answers).

	LTMI	LTMI-LGKD
Method 1 (M1)	56	66
Method 2 (M2)	61	69

Table 6: Human evaluation on 100 sampled responses on VisDial val v1.0. M1: percentage of responses pass the Turing Test. M2: percentage of responses evaluated better than or equal to human responses.

4 Related Work

Visual Dialog Recent visual dialog models focus on the intersection of questions, history and images. How to locate the related visual objects is quite importance. MN (Das et al., 2017), HCIAE (Lu et al., 2017), CorefNMN (Kottur et al., 2018), CoAtt (Wu et al., 2018), RvA (Niu et al., 2019), DVAN (Guo et al., 2019b) utilize kinds of attention mechanisms as the backbone to locate the related visual objects. VisualBERT (Murahari et al., 2020) and VDBERT (Wang et al., 2020) exploit large extra datasets to explore in visual dialog via pretraining language models. GNN-EM (Zheng et al., 2019), FGA (Schwartz et al., 2019), DualVD (Jiang et al., 2020b), CAG (Guo et al., 2020) and KBGN (Jiang et al., 2020a) utilize graph neural networks to obtain the final representation of visual objects. In this paper, we utilize answer-aware knowledge distillation to learn to ground visual objects based on a teacher-student framework.

Knowledge Distillation Knowledge distillation (Hinton et al., 2015; Gou et al., 2020; Mirzadeh et al., 2020; Romero et al., 2014; Liu et al., 2019; Jiao et al., 2019) has been widely used in different fields of artificial intelligence, including visual recognition, speech, recognition,

natural language processing, and recommendation systems. Zagaruyko and Komodakis (2016) improve the performance of a student CNN network by forcing it to mimic the attention maps of a powerful teacher network via properly defining attention for convolutional neural networks. Tian et al. (2020) propose a method to construct a response-anticipated memory to contain document information that is potentially more important in generating responses via knowledge distillation. In this paper, we propose an answer-aware knowledge distillation to teach the student model to learn to ground visual objects.

5 Conclusion

In this paper, we propose a novel approach to learn to ground visual objects for visual dialog via answer-aware knowledge distillation (LGKD), which is achieved using a teacher-student framework. Specifically, the student is as the same as existing visual dialog models which take questions, history and images as inputs. The teacher equipped with answers additionally learns how to ground answer-aware visual objects and then guides the student via knowledge distillation. Experimental results on two large-scale datasets show that our approach improves the previous models by a significant margin.

References

- Shubham Agarwal, Trung Bui, Joon-Young Lee, Ioannis Konstas, and Verena Rieser. 2020. History for visual dialog: Do we really need it? *arXiv preprint arXiv:2005.07493*.
- Peter Anderson, Basura Fernando, Mark Johnson, and Stephen Gould. 2016. SPICE: Semantic propositional image caption evaluation. *Adaptive Behavior*, 11(4):382–398.
- Peter Anderson, Xiaodong He, Chris Buehler, Damien Teney, Mark Johnson, Stephen Gould, and Lei Zhang. 2018. Bottom-up and top-down attention for image captioning and visual question answering. In *Proceedings of the IEEE Conference on Computer Vision and Pattern Recognition*, pages 6077–6086.
- Feilong Chen, Xiuyi Chen, Fandong Meng, Peng Li, and Jie Zhou. 2021a. Gog: Relation-aware graph-over-graph network for visual dialog. *arXiv preprint arXiv:2109.08475*.
- Feilong Chen, Fandong Meng, Xiuyi Chen, Peng Li, and Jie Zhou. 2021b. Multimodal incremental transformer with visual grounding for visual dialogue generation. *arXiv preprint arXiv:2109.08478*.
- Feilong Chen, Fandong Meng, Jiaming Xu, Peng Li, Bo Xu, and Jie Zhou. 2020. DMRM: A dual-channel multi-hop reasoning model for visual dialog. *Thirty-Fourth AAAI Conference on Artificial Intelligence*.
- Marcella Cornia, Matteo Stefanini, Lorenzo Baraldi, and Rita Cucchiara. 2020. Meshed-memory transformer for image captioning. In *Proceedings of the IEEE/CVF Conference on Computer Vision and Pattern Recognition*.
- Abhishek Das, Satwik Kottur, Khushi Gupta, Avi Singh, Deshraj Yadav, José MF Moura, Devi Parikh, and Dhruv Batra. 2017. Visual dialog. In *Proceedings of the IEEE Conference on Computer Vision and Pattern Recognition*, pages 326–335.
- Zhe Gan, Yu Cheng, Ahmed El Kholy, Linjie Li, Jingjing Liu, and Jianfeng Gao. 2019. Multi-step reasoning via recurrent dual attention for visual dialog. In *Proceedings of the 57th Annual Meeting of the Association for Computational Linguistics*, pages 6463–6474.
- Haoyuan Gao, Junhua Mao, Jie Zhou, Zhiheng Huang, Lei Wang, and Wei Xu. 2015. Are you talking to a machine? dataset and methods for multilingual image question. In *Advances in Neural Information Processing Systems*, pages 2296–2304.
- Mehdi Ghanimifard and Simon Dobnik. 2019. What goes into a word: generating image descriptions with top-down spatial knowledge. In *Proceedings of the 12th International Conference on Natural Language Generation*, pages 540–551.
- Jianping Gou, Baosheng Yu, Stephen John Maybank, and Dacheng Tao. 2020. Knowledge distillation: A survey. *arXiv preprint arXiv:2006.05525*.
- Dalu Guo, Chang Xu, and Dacheng Tao. 2019a. Image-question-answer synergistic network for visual dialog. In *Proceedings of the IEEE Conference on Computer Vision and Pattern Recognition*, pages 10434–10443.
- Dan Guo, Hui Wang, and Meng Wang. 2019b. Dual visual attention network for visual dialog. pages 4989–4995.
- Dan Guo, Hui Wang, Hanwang Zhang, Zheng-Jun Zha, and Meng Wang. 2020. Iterative context-aware graph inference for visual dialog. In *Proceedings of the IEEE/CVF Conference on Computer Vision and Pattern Recognition*, pages 10055–10064.
- Kaiming He, Xiangyu Zhang, Shaoqing Ren, and Jian Sun. 2016. Deep residual learning for image recognition. *Proceedings of the IEEE Conference on Computer Vision and Pattern Recognition*, pages 770–778.
- Geoffrey Hinton, Oriol Vinyals, and Jeff Dean. 2015. Distilling the knowledge in a neural network. *arXiv preprint arXiv:1503.02531*.
- Qingbao Huang, Jielong Wei, Yi Cai, Changmeng Zheng, Junying Chen, Ho-fung Leung, and Qing Li. 2020. Aligned dual channel graph convolutional network for visual question answering. In *Proceedings of the 58th Annual Meeting of the Association for Computational Linguistics*, pages 7166–7176.
- Xiaoze Jiang, Siyi Du, Zengchang Qin, Yajing Sun, and Jing Yu. 2020a. KBGN: Knowledge-bridge graph network for adaptive vision-text reasoning in visual dialogue. *Proceedings of the 28th ACM International Conference on Multimedia*.
- Xiaoze Jiang, Jing Yu, Zengchang Qin, Yingying Zhuang, Xingxing Zhang, Yue Hu, and Qi Wu. 2020b. DualVD: An adaptive dual encoding model for deep visual understanding in visual dialogue. In *AAAI*, volume 1, page 5.
- Xiaoze Jiang, Jing Yu, Yajing Sun, Zengchang Qin, Zihao Zhu, Yue Hu, and Qi Wu. 2020c. DAM: Deliberation, abandon and memory networks for generating detailed and non-repetitive responses in visual dialogue. *arXiv preprint arXiv:2007.03310*.
- Xiaoqi Jiao, Yichun Yin, Lifeng Shang, Xin Jiang, Xiao Chen, Linlin Li, Fang Wang, and Qun Liu. 2019. Tinybert: Distilling bert for natural language understanding. *arXiv preprint arXiv:1909.10351*.
- Satwik Kottur, José M. F. Moura, Devi Parikh, Dhruv Batra, and Marcus Rohrbach. 2018. Visual coreference resolution in visual dialog using neural module networks. *ArXiv*, abs/1809.01816.

- Ranjay Krishna, Yuke Zhu, Oliver Groth, Justin Johnson, Kenji Hata, Joshua Kravitz, Stephanie Chen, Yannis Kalantidis, Li-Jia Li, David A. Shamma, Michael S. Bernstein, and Li Fei-Fei. 2017. Visual genome: Connecting language and vision using crowdsourced dense image annotations. *International Journal of Computer Vision*, 123(1):32–73.
- Yann LeCun, Yoshua Bengio, and Geoffrey Hinton. 2015. Deep learning. *nature*, 521(7553):436–444.
- Linjie Li, Zhe Gan, Yu Cheng, and Jingjing Liu. 2019. Relation-aware graph attention network for visual question answering. In *Proceedings of the IEEE International Conference on Computer Vision*, pages 10313–10322.
- Junjie Liu, Dongchao Wen, Hongxing Gao, Wei Tao, Tse-Wei Chen, Kinya Osa, and Masami Kato. 2019. Knowledge representing: Efficient, sparse representation of prior knowledge for knowledge distillation. In *Proceedings of the IEEE Conference on Computer Vision and Pattern Recognition Workshops*, pages 0–0.
- Jiasen Lu, Anitha Kannan, Jianwei Yang, Devi Parikh, and Dhruv Batra. 2017. Best of both worlds: Transferring knowledge from discriminative learning to a generative visual dialog model. In *Advances in Neural Information Processing Systems*, pages 314–324.
- Jiasen Lu, Jianwei Yang, Dhruv Batra, and Devi Parikh. 2016. Hierarchical question-image co-attention for visual question answering. In *Advances In Neural Information Processing Systems*, pages 289–297.
- Seyed Iman Mirzadeh, Mehrdad Farajtabar, Ang Li, Nir Levine, Akihiro Matsukawa, and Hassan Ghasemzadeh. 2020. Improved knowledge distillation via teacher assistant. In *Proceedings of the AAAI Conference on Artificial Intelligence*, volume 34, pages 5191–5198.
- Vishvak Murahari, Dhruv Batra, Devi Parikh, and Abhishek Das. 2020. Large-scale pretraining for visual dialog: A simple state-of-the-art baseline. *Proceedings of the European Conference on Computer Vision*.
- Van-Quang Nguyen, Masanori Suganuma, and Takayuki Okatani. 2020. Efficient attention mechanism for visual dialog that can handle all the interactions between multiple inputs. *Proceedings of the European Conference on Computer Vision*.
- Yulei Niu, Hanwang Zhang, Manli Zhang, Jianhong Zhang, Zhiwu Lu, and Ji-Rong Wen. 2019. Recursive visual attention in visual dialog. In *Proceedings of the IEEE Conference on Computer Vision and Pattern Recognition*, pages 6679–6688.
- Jiaxin Qi, Yulei Niu, Jianqiang Huang, and Hanwang Zhang. 2020. Two causal principles for improving visual dialog. *Proceedings of the IEEE Conference on Computer Vision and Pattern Recognition*.
- Mengye Ren, Ryan Kiros, and Richard Zemel. 2015a. Exploring models and data for image question answering. In *Advances in Neural Information Processing Systems*, pages 2953–2961.
- Shaoqing Ren, Kaiming He, Ross Girshick, and Jian Sun. 2015b. Faster R-CNN: Towards real-time object detection with region proposal networks. In *Advances in Neural Information Processing Systems*, pages 91–99.
- Adriana Romero, Nicolas Ballas, Samira Ebrahimi Kahou, Antoine Chassang, Carlo Gatta, and Yoshua Bengio. 2014. Fitnets: Hints for thin deep nets. *arXiv preprint arXiv:1412.6550*.
- Idan Schwartz, Seunghak Yu, Tamir Hazan, and Alexander G Schwing. 2019. Factor graph attention. In *Proceedings of the IEEE Conference on Computer Vision and Pattern Recognition*, pages 2039–2048.
- Ilya Sutskever, Oriol Vinyals, and Quoc V Le. 2014. Sequence to sequence learning with neural networks. *arXiv preprint arXiv:1409.3215*.
- Zhiliang Tian, Wei Bi, Dongkyu Lee, Lanqing Xue, Yiping Song, Xiaojiang Liu, and Nevin L Zhang. 2020. Response-anticipated memory for on-demand knowledge integration in response generation. *arXiv preprint arXiv:2005.06128*.
- Ashish Vaswani, Noam Shazeer, Niki Parmar, Jakob Uszkoreit, Llion Jones, Aidan N Gomez, Łukasz Kaiser, and Illia Polosukhin. 2017. Attention is all you need. In *Advances in neural information processing systems*, pages 5998–6008.
- Yue Wang, Shafiq Joty, Michael R Lyu, Irwin King, Caiming Xiong, and Steven CH Hoi. 2020. VD-BERT: A unified vision and dialog transformer with bert. *arXiv preprint arXiv:2004.13278*.
- Qi Wu, Peng Wang, Chunhua Shen, Ian Reid, and Anton van den Hengel. 2018. Are you talking to me? reasoned visual dialog generation through adversarial learning. In *Proceedings of the IEEE Conference on Computer Vision and Pattern Recognition*, pages 6106–6115.
- Kelvin Xu, Jimmy Ba, Ryan Kiros, Kyunghyun Cho, Aaron Courville, Ruslan Salakhudinov, Rich Zemel, and Yoshua Bengio. 2015. Show, attend and tell: Neural image caption generation with visual attention. In *Proceedings of International Conference on Machine Learning*, pages 2048–2057.
- Sergey Zagoruyko and Nikos Komodakis. 2016. Paying more attention to attention: Improving the performance of convolutional neural networks via attention transfer. *arXiv preprint arXiv:1612.03928*.
- Zilong Zheng, Wenguan Wang, Siyuan Qi, and Song-Chun Zhu. 2019. Reasoning visual dialogs with structural and partial observations. In *Proceedings of the IEEE Conference on Computer Vision and Pattern Recognition*, pages 6669–6678.